



## Experiment Report Form



	<p><b>Experiment title:</b> Relating brain function to structure with subcellular resolution</p>	<p><b>Experiment number:</b> LS2918</p>
<p><b>Beamline:</b> ID16A</p>	<p><b>Date of experiment:</b> from: 4<sup>th</sup> February 2021 to: 9<sup>th</sup> February 2021</p>	<p><b>Date of report:</b> 24<sup>th</sup> February 2021</p>
<p><b>Shifts:</b> 15</p>	<p><b>Local contact(s):</b> Alexandra Pacureanu and Peter Cloetens</p>	<p><i>Received at ESRF:</i></p>
<p><b>Names and affiliations of applicants (* indicates experimentalists):</b></p> <p><b>Main proposer:</b> Carles Bosch, The Francis Crick Institute, London, UK</p> <p><b>Co-proposers:</b> Andreas Schaefer, The Francis Crick Institute, London, UK Alexandra Pacureanu, ESRF, Grenoble, France</p>		

## Report:

### Introduction

The purpose of this proposal was to link *in vivo* function to subcellular anatomical structure in the mouse brain by integrating X-ray nanoholotomography (XNH) in a correlative multimodal imaging pipeline. The neural circuit of interest was the glomerular column in the mouse olfactory bulb, a modular and compact circuit containing the first synapses in the olfactory sensory pathway.

For this purpose we designed an experiment in which we recorded neural activity *in vivo* while a panel of 48 monomolecular odorants was presented to an anesthetized mouse using a custom odour delivery setup<sup>1</sup>. The mouse expressed the Ca<sup>2+</sup>-sensitive fluorescent indicator GCaMP6f under the Tbet promoter, revealing the neural activity of all projection neurons in the olfactory bulb under a 2-photon microscope. Six planes were imaged covering a (500 μm)<sup>3</sup> volume in the surroundings of a genetically-tagged glomerulus (MOR174/9-eGFP), enabling replicating this experiment by targeting the same genetically-tagged region in a different animal.

After the functional recording of temporal cell activation responses to the different odorants, a fluorescent blood vessel reporter (sulforhodamine 101) was intraperitoneally administered and we recorded a spatially-detailed dataset in the same *in vivo* 2-photon setup covering the same (500 μm)<sup>3</sup> volume with (0.358\*0.358\*5) μm<sup>3</sup> voxels. The brain region was then dissected, stained with an standard EM protocol<sup>2</sup> and imaged with full-field X-ray tomography at Diamond I13-2 (proposal MT2024) and at PSI TOMCAT (proposal 20190417).

The X-ray tomograms revealed subcellular details including the positions of cell nuclei and blood vessels. This information allowed identifying multiple landmarks in the synchrotron and 2-photon datasets, ultimately allowing to warp the latter into the former space coordinates<sup>3</sup> and identify ~100 out of the 277 cell bodies functionally imaged *in vivo*.

The stained tissue section, initially of ~3\*3\*0.6mm, was trimmed to an ID16A-compatible size in a way that it would retain the *in vivo* imaged region, thereby resulting in a parallelogrammic prism (**Fig 4a-c**) sitting on a synchrotron holder and reembedded in a droplet of resin so as to protect the specimen and provide a smooth air-sample interface without edges. This specimen was then scanned with a lab X-ray CT (Zeiss Versa 510) and shipped to ESRF. The lab X-ray tomogram could be warped to the synchrotron X-ray tomogram, revealing the positions of the *in vivo* recorded cells in the trimmed specimen.

The beamtime experiment was conducted remotely, with the presence in the beamline of the co-proposer A.P. and the local contact P.C. The main proposer C.B., co-proposer A.S. and the PhD candidate Yuxin Zhang assisted remotely.

At the beginning of the beamtime we agreed on:

#### Checkpoints:

1. Find distinguishable features in the specimen and identify region of interest
2. Find optimal imaging settings
3. Verify stitching of adjacent tiles is feasible
4. Scan through all tiles routinely

#### Channels of communication:

- Specific channel on slack
- Specific videoconference room on zoom
- Log book and folder to store preliminary images on google drive

#### Background information:

- Synchrotron X-ray tomography with annotated regions of interest ([link](#))
- Lab X-ray tomography of the trimmed sample with annotated regions of interest ([link](#))

#### Data transfer protocols:

- ssh
- globus

Goals:

- Acquire from below the mitral cell layer (retrieving all mitral cells) up to ~30% of the top layer of glomeruli
- Obtain preliminary insights to unforeseen bottlenecks to inform future improvements

**Results**

Orientation in the specimen and identifying region of interest

The location of the prism in the sample could be identified macroscopically by comparing the overall shape observed under a magnifying lens to the expected cartography. An asymmetrical resin edge signaled the specimen's orientation, and guided its positioning closest to the detector (**Fig 1**). Macroscopic sample orientation could be improved by designing asymmetrical holders or etching unequivocal marks that could unambiguously guide the location of the region of interest as close as possible to the detector.

The lab X-ray CT dataset was virtually resliced using Fiji<sup>4</sup> in the orientation expected to be seen from the detector and in the perpendicular orientation, to anticipate the image patterns that we expected to obtain (**Fig 1**).

The sample was imaged in cryogenic conditions using liquid N<sub>2</sub>.

Initial scans targeted the top of the sample, corresponding to the brain's surface. Asymmetrical features in the surface provided unique patterns that matched with the expected images (**Fig 2**), confirming the initial coarse positioning was correct.

mounting sample - macroscopic ROI location

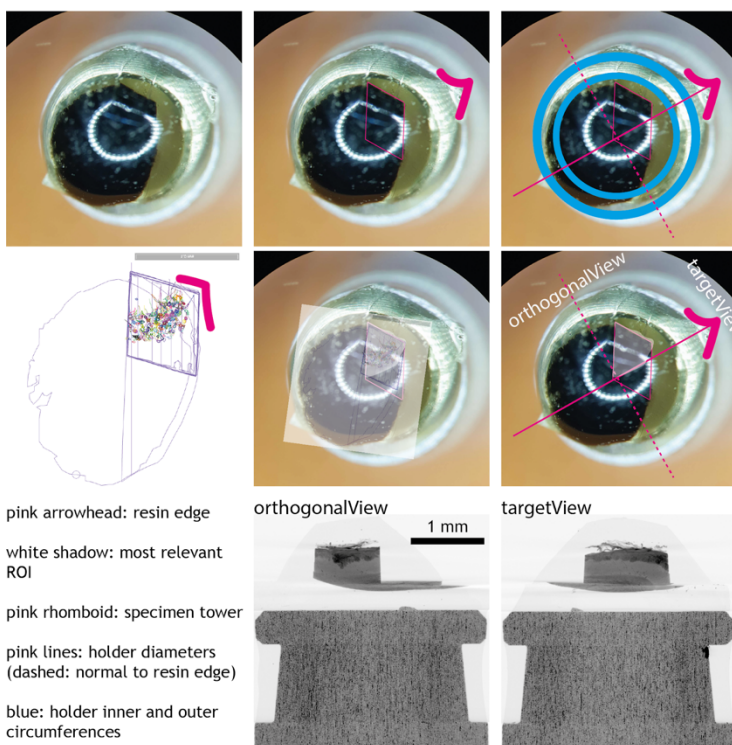


**Figure 1. Sample positioning in the chamber**

The location of the prism in the sample was guided by a resin edge (purple). Holder internal and external diameters are marked in the top-right panel in blue. The prism was located proximal to the detector, and expected views were generated from a lab-source CT dataset.

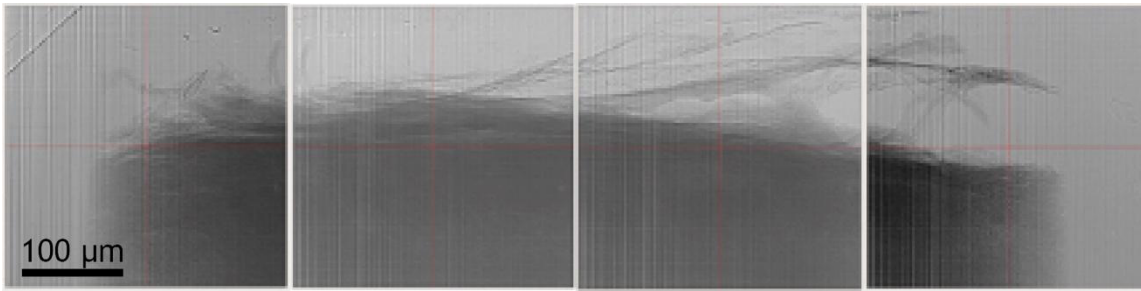


**Figure 2. Surface of the sample revealed by single projections in the beamline setup**

A fast scan provided evidence of asymmetrical features in the sample's surface that matched the expected view, thereby confirming coarse orientation was correct.

In order to map the regions of interest we proceeded to identify the vertices of the parallelogram. The sample sides at the proximal edge could be oriented parallel to the beam by monitoring the absorption in the lateral edge as the sample rotated. Being the sample a prism of known face angles, this approach provided the location in beamline coordinates of the proximal vertex, and consequently the location in beamline coordinates of the entire specimen map (**Fig 3**).

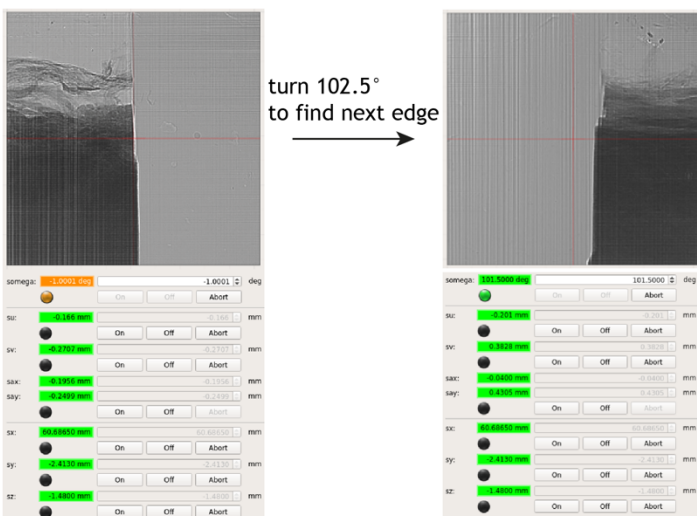


**Figure 3. Location of the sample's vertex that was closest to the detector**

### Imaging settings

Transmission at 17 keV was ~14% at 0° (flat field scans obtained out of the resin).

This transmission was lower than previously obtained with similarly stained specimens, attributable to its larger dimensions (Table 1) but within the acceptable range.

Specimen name	Size	Beam energy	Transmission
<b>C432</b>	Parallelogrammic prism smallD = 965 μm largeD = 1230 μm	17 keV	14 %
<b>C417</b>	Cylinder D = 800 μm	33 keV	63 %
<b>Cortex</b>	Cylinder D = 750 μm	17 keV	30 %

**Table 1. X-ray transmission of metal-stained mouse brain tissue specimens at ID16A.**

A fast tomography containing the proximal vertex of the specimen was acquired using 1600 projections and 0.3 s/projection. The features resolved in this scan also enabled identifying known soft tissue landmarks by comparing to the previously obtained lab and synchrotron full-field tomographies, and therefore providing the final evidence for the location of the regions of interest in beamline coordinates.

The total duration of each holotomo scan was 3h15min.

### Tile configuration and data acquisition

Individual reconstructed tiles were cylinders of 3216\*3216 pixels diameter and height, with a pixel size of 100nm. Data quality in the tile was expected to be of two types: highest resolution in the central 2000\*2000 pixel cylinder, and lower resolution in the outer shell (**Fig 4d**). Tiles were positioned so highest-resolution zones would be adjacent and covering two layers in z. Up to 28 tiles were expected to be obtained during the assigned beamtime. The desired tile arrangement was devised and tiles ranked ensuring that tissue containing *in vivo* recorded cells and their expected dendrites would be imaged earlier in the beamtime in case unforeseen circumstances would curtail the experiment (**Fig 4e**).

Before launching the scan array, each sample vertex was revisited and ensured that sample borders aligned to 0° and 105°. A custom script was then developed to configure the consecutive acquisition of all 28 tiles.

As soon as two adjacent tiles were first acquired, they were reconstructed and preliminary analysis confirmed enough overlap was present to be stitched successfully and that lateral dendrites could be segmented (**Fig 4f-i**).

During the beamtime there was an 8h long beam loss.

We could successfully collect data for 28 adjacent tiles covering  $\sim 400*700*800 \mu\text{m}^3$  of mouse brain tissue.

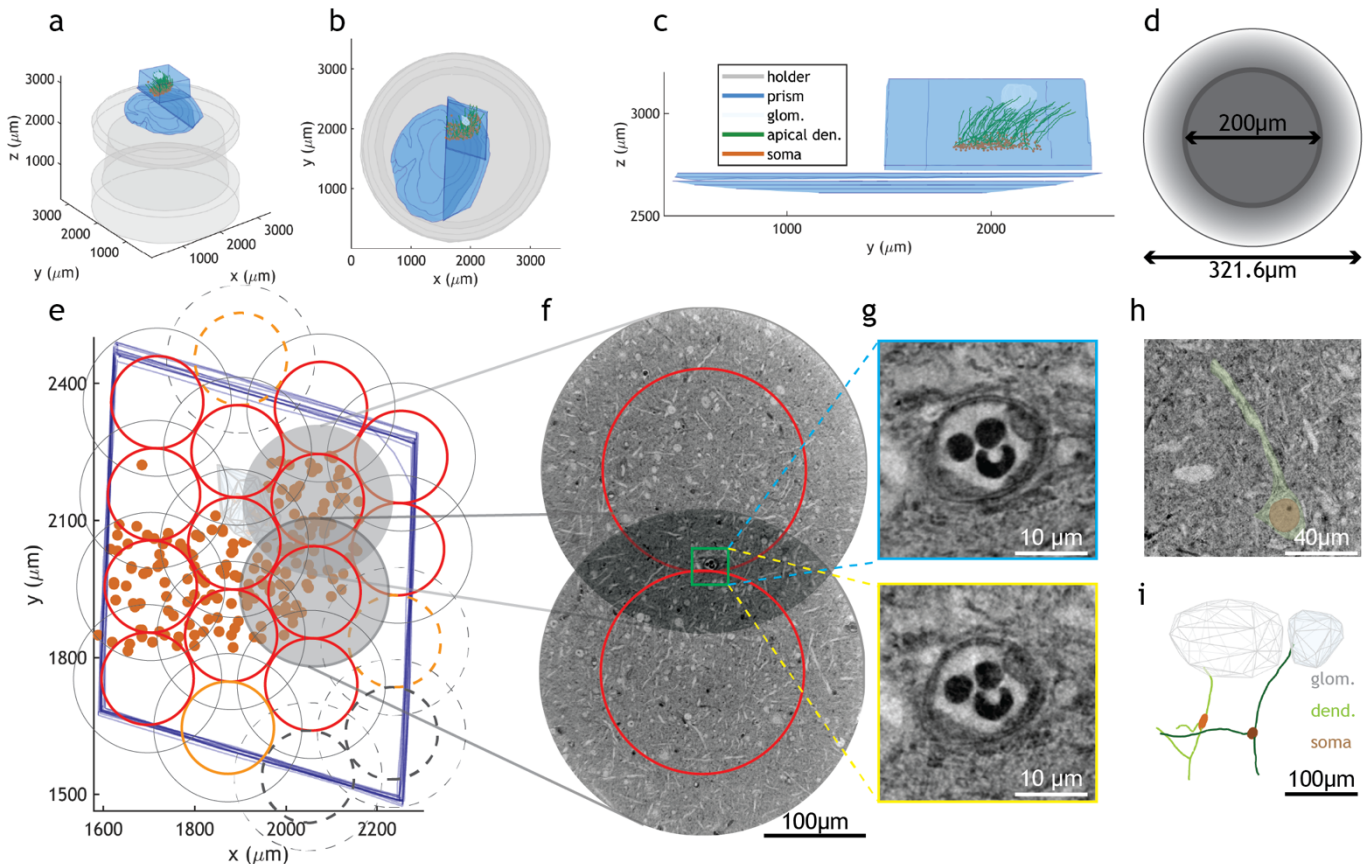


**Figure 4. Sample properties, tiling plan, stitching and preliminary annotations**

(a-c) Side (a), top (b) and front (c) views of the sample. The sample consisted of stained mouse brain tissue (blue) trimmed into a prism and embedded on top of a synchrotron aluminium holder (gray). Prior to beamtime, regions of interest including *in vivo* imaged cell bodies (brown), their upward projecting apical dendrites (green) and a genetically labelled glomerulus (white) were localized and annotated in the prism using other correlated light and synchrotron X-ray tomography imaging data. (d) Tile resolution is best at its core. (e) The *in vivo* imaged volume was scanned in two stacked layers of 14 tiles each (acquired tiles shown in solid lines). Tiles were ranked by priority (“essential” shown in red, “desirable” in orange, “optional” in black). (f-g) The overlap between adjacent tiles is both large (f) and feature-rich (g), therefore stitching is possible. (h-i) Lateral dendrites (green, nucleus in brown) are resolved (h) and can be followed until exiting the tile (i). *glom. is glomerulus, den. is dendrite*



## Data analysis

Tomograms are being reconstructed at ESRF and transferred to the Francis Crick Institute for storage and analysis. They will be stitched using a non-rigid algorithm developed for synchrotron X-ray tomography<sup>5</sup>.

Follow-up analysis will have two main parts:

- The tiles will be stitched generating a joint continuous dataset, where all dendritic branches of *in vivo* imaged neurons will be traced.
- The specimen will be milled into multiple pillars, each containing a volume  $> (200\mu\text{m})^3$ . Those pillars will be imaged at synaptic resolution with volume electron microscopy.

All analyses will be warped to a common 3D framework, thereby informing of the structure of the inhibitory network mediated by granule cell interneurons that links projection neurons of known physiological profile.

## **Discussion**

The purpose of this proposal was to link *in vivo* function to subcellular anatomical structure in the mouse brain by integrating X-ray nanoholotomography (XNH) in a correlative multimodal imaging pipeline. We acquired with XNH 28 adjacent tiles covering  $\sim 400 \times 700 \times 800 \mu\text{m}^3$  of mouse brain tissue containing  $\sim 100$  neurons of known physiological activity. Because complete glomerular columns are embedded in this tissue, we are certain we will be able to group projection neurons with known physiology by the glomerular column they belong to, thereby grouping sister mitral cells together and thus describing input-output relations in this mammalian neuronal circuit. We expect being able to trace a large fraction of the lateral dendrites of all recorded projection neurons, responsible for computational interactions between glomerular columns. We plan to follow up this study with synapse-resolution volume electron microscopy of narrower regions of interest in the external plexiform layer, that will characterize the connectivity patterns along these lateral dendrites of neurons with known physiology. These results will raise key insights on how information is processed in a mouse's brain. During the preparation of the correlative workflow we have gathered insights on how to improve certain steps such as region targeting, sample cutting and mounting for optimal data quality. We have also concluded that for the combination of sample staining level and meaningful sample size for this experiment, it would be more suitable to image at 33.6 keV. Therefore a replication of this experiment with a second sample would simultaneously provide sufficient data for a solid publication and enable us to implement the gained insight into the optimization of the workflow, which will be useful for other ESRF users as well.

## **References**

- 1 Erskine, A., Ackels, T., Dasgupta, D., Fukunaga, I. & Schaefer, A. T. Mammalian olfaction is a high temporal bandwidth sense. *bioRxiv*, doi:<https://doi.org/10.1101/570689> (2019).
- 2 Pallotto, M., Watkins, P. V., Fubara, B., Singer, J. H. & Briggman, K. L. Extracellular space preservation aids the connectomic analysis of neural circuits. *Elife* **4**, doi:10.7554/eLife.08206 (2015).
- 3 Bosch, C. *et al.* Functional and multiscale 3D structural investigation of brain tissue through correlative *in vivo* physiology, synchrotron micro-tomography and volume electron microscopy. *bioRxiv*, doi:<https://doi.org/10.1101/2021.01.13.426503> (2021).
- 4 Schindelin, J. *et al.* Fiji: an open-source platform for biological-image analysis. *Nat Methods* **9**, 676-682, doi:10.1038/nmeth.2019 (2012).
- 5 Miettinen, A., Oikonomidis, I. V., Bonnin, A. & Stampanoni, M. NRStitcher: non-rigid stitching of terapixel-scale volumetric images. *Bioinformatics* **35**, 5290-5297, doi:10.1093/bioinformatics/btz423 (2019).